J. Fluid Mech. (1983), *vol.* 134, *pp.* 259–275
Printed in Great Britain

Free-surface flows related to breaking waves

By MARTIN GREENHOW†
Department of Applied Mathematics and Theoretical Physics, University of Cambridge, Silver Street, Cambridge CB3 9EW

(Received 6 August 1982 and in revised form 29 April 1983)

Using the semiLagrangian approach of John (1953), both Longuet-Higgins (1982) and New (1983) have proposed simple analytical models of the underside or loop of a plunging breaking wave. Although New's ellipse model appears to be remarkably accurate both in profile and free-surface particle dynamics for a limited region of the loop, both of the loop models are shown to be deficient because neither correctly accounts for the rest of the wave. On the other hand, Longuet-Higgins (1983) gives a semiLagrangian representation of the Dirichlet hyperbola, previously shown to be relevant to the jet of fluid ejected from the top of a breaking wave (see Longuet-Higgins 1980). We show that both this jet flow and the ellipse model of New describing the loop are, for large time, complementary solutions of the same free surface equation. This in turn suggests solutions which combine both the jet and the loop, to give a much more complete model of the entire overturning region not too far from the wave crest, and which has approximately correct free-surface particle velocities and accelerations.

1. Introduction

The purpose of this paper is to explore further some simple analytical free-surface flows valid in the absence of gravity which may be related to the plunging of a breaking wave. Using the semiLagrangian approach of John (1953) described in §2, Longuet-Higgins (1982) presents a simple cubic model of the underside, or loop, of a plunging breaker, while Longuet-Higgins (1983) gives a semiLagrangian representation of the jet (a Dirichlet hyperbola) which is ejected from the crest of a breaking wave. New (1983) also presents a model of the loop (the $\sqrt{3}$-ellipse) in which the free surface fluid particles have a realistic rotation around the loop. The aim of this paper is to build upon these solutions to produce a combined jet and loop flow in which there are no non-annulled singularities within the fluid, and for which the fluid velocities and accelerations are qualitatively correct.

Section 3 discusses these previously known solutions with a view to seeing if their shortcomings might be overcome by some sort of modification or extension. For example, Longuet-Higgins (1982) shows that the cubic solution has another surface of vanishing pressure which approximately accommodates the rear of the wave and can be used to justify the accuracy of the model's fit with the loop of the wave. Does New's ellipse, with its superior modelling of the particle dynamics within the loop, also have such an approximation to the rear of the wave? Section 3 shows that it does not. However, the main conclusion relevant to the rest of the paper is as follows: if the rear of the wave is to be modelled by another zero-pressure surface, then in

† Present address: Department of Ocean Engineering, Massachusetts Institute of Technology, Cambridge, MA 02139

order for this surface to connect up with the loop region the pressure gradient at the point of connection must vanish. This implies that the particle acceleration must vanish here ($= g$ in a fixed frame), which is not observed in numerical calculations of breaking waves until the jet is very well formed. This conclusion was also drawn by Longuet-Higgins (1982), but its implication, that a model of the loop part of the wave must accommodate the jet of the wave *a priori* (and not rely on other $p = 0$ surfaces), is exploited in the present paper.

Section 4 discusses the semiLagrangian representation of the Dirichlet hyperbola (see Longuet-Higgins 1983), which is strictly valid only within the jet region. Nevertheless it is shown that both the Dirichlet hyperbola and the ellipse of New are both solutions of John's free surface equation:

$$z_{tt} = \mathrm{i}rz_{\omega}, \tag{1.1}$$

with the r-functions for both models having the same behaviour for large time. Since the former is a jet flow while the latter describes a loop, it may be possible to combine both flows to describe a large part of the breaking wave's overturning region, provided that singularities within the fluid are annulled. Conversely (1.1) may be used to generate combined loop and jet flows which do not rely on other $p = 0$ surfaces to model the rear of the wave and consequently avoid the difficulty arising in previous loop models. This is the approach of the present paper, and in preparation for this some necessary asymptotic solutions and relations are given in §5. Section 6 gives possible solutions to the combined loop and jet flow with qualitatively correct velocities and accelerations, and suitably annulled singularities, at least in the large time limit. When compared with numerically generated breaking waves, the agreement is about as good as can be expected since the proposed analytic model only includes gravity in a non-essential way. Finally, §7 is a comparison of the r-function used to generate the solution, with the computational r-function of the numerically generated breaking waves. This gives support to the applicability of the semiLagrangian technique and the present solution, although some shortcomings of the model r-function are also illuminated.

2. John's formalism

For a free-surface flow we suppose that on the free surface the particles are labelled by a real parameter ω which is constant following a particle, and is thus termed a semiLagrangian description by Longuet-Higgins (1982). Assuming gravity to act in the positive x-direction, John (1953) then writes the free-surface equation as:

$$z_{tt} - g = \mathrm{i}r(\omega, t)\, z_{\omega}, \tag{2.1}$$

where $r(\omega, t)$ is a real function of ω and t.

In case of a gravity-free flow (or if we take axes moving with downward acceleration g) we have

$$z_{tt} = \mathrm{i}r(\omega, t)\, z_{\omega}, \tag{2.2}$$

which has solution z_1 say. Hence a solution to (2.1) can be formed from z_1 by the addition of $\frac{1}{2}gt$, and is said to include gravity in a non-essential way.

A great advantage of using the semiLagrangian description is that the free surface is characterized by a *linear* equation. Hence any two solutions satisfying (2.1) or (2.2) with the same function $r(\omega, t)$ may be added together to give a third solution of the equation: we call them complementary solutions.

On the free surface we must have the pressure and its material derivative vanishing:

$$p = 0, \tag{2.3}$$

$$\frac{\mathrm{D}p}{\mathrm{D}t} = 0. \tag{2.4}$$

When ω is real (2.3) and (2.4) are automatically satisfied. There may be, however, other surfaces in the ω-plane satisfying (2.3) and (2.4) given by the roots of

$$-2p = (\chi_t + \chi_t^*) + z_t(\omega^*)\, z_t^*(\omega) - g(z+z^*) \\ -2f - [z_t(\omega)\, z_t^*(\omega) + z_t(\omega^*)\, z_t^*(\omega^*)] = 0, \tag{2.5}$$

$$\frac{\mathrm{D}p}{\mathrm{D}t} = p_t + Kp_\omega + K^* p_{\omega^*} = 0, \tag{2.6}$$

as in Longuet-Higgins (1982), where f is an arbitrary function of time,

$$\chi = \int^{\omega} z_\omega(\omega)\, z_t^*(\omega)\, \mathrm{d}\omega, \tag{2.7}$$

is the velocity potential, and

$$K = \frac{\mathrm{D}\omega}{\mathrm{D}t} = \frac{z_t(\omega^*) - z_t(\omega)}{z_\omega}. \tag{2.8}$$

Lastly, within the fluid domain we require that χ has no singularities that are not annulled. Thus if $z_\omega = 0$ then $z_{\omega t}^*(\omega)$ must vanish at the same point within the fluid domain, in which case the singularity is annulled.

This paper describes flows that do not contain gravity in an essential way and are solutions of (2.2). The reason why such flows may be relevant to the crest region of a breaking wave is that numerical solutions indicated that the jet is in free fall, whilst for the loop the free-surface particle accelerations can be 2 or 3 g. Consequently, for a well-overturned wave it may be approximately correct to ignore gravity over a region not too far from the wave crest.

3. Discussion of the loop models of Longuet-Higgins and New

In this section we ask whether the solutions of Longuet-Higgins (1982) and New (1983), which are proposed models for the underside or loop of a plunging breaker, can be extended or modified to include the rest of the wave. Longuet-Higgins proposes a simple self-similar cubic solution which fits the loop remarkably accurately and partially justifies the accuracy of the fit by showing that the rear of the wave is approximately accounted for by another surface of vanishing pressure. New objects that the free-surface particles of the cubic do not have the systematic rotation up into the jet observed in breaking waves. (We also note that the surface particle accelerations of the cubic are directed into the fluid implying that the proposed fluid domain has negative pressure. Other cubic solutions given in Longuet-Higgins (1976) do not have this defect, but still do not have the correct rotation.) New's ellipse model incorporates this rotation and also has surface-particle accelerations directed out of the fluid as required: thus as a model for the loop region the ellipse appears to be very good for both profiles and velocities of the free-surface. It is natural to ask if this accuracy is justified by other $p = 0$ surfaces as in the cubic model of

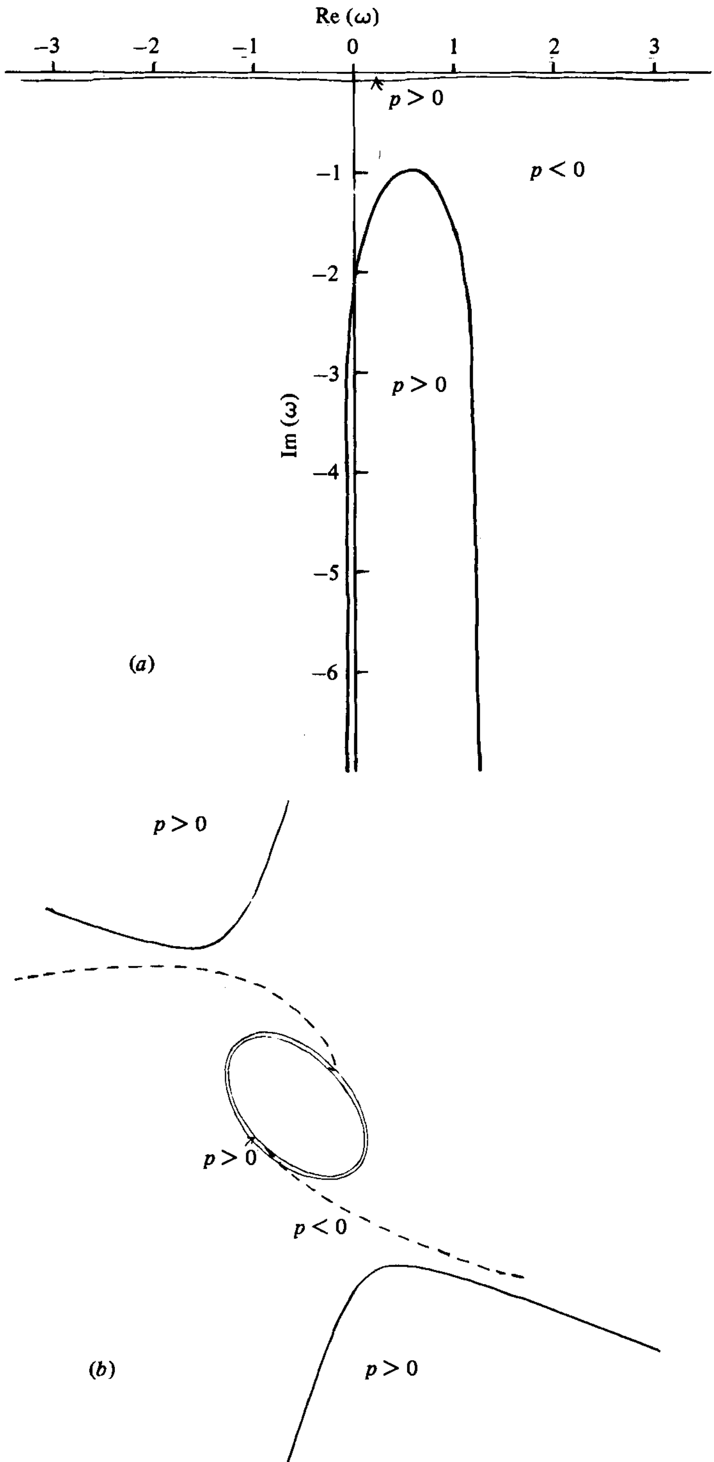

FIGURE 1. (a) $p = 0$ surfaces in the ω-plane for the ellipse solution of New. One surface lies close to the ellipse solution given by ω real, and gives some support to New's arguments. $t = 1$. The surfaces are periodically repeated under $\mathrm{Re}\,(\omega) \rightarrow \mathrm{Re}\,(\omega) + 2n\pi$, n integer. (b) $p = 0$ surfaces in the physical z-plane. The dotted line shows the numerical results of Vinje & Brevig.

Longuet-Higgins, which account for the rear of the wave. Figure 1 shows the other $p = 0$ surfaces (generated by putting New's solution into (2.5) and solving numerically) do not pass near the rear of the wave and consequently provide no justification for the ellipse's accuracy. (One $p = 0$ surface runs close to the elliptic free surface and gives some support to the arguments presented by New (1983)). Also the reason why the eccentricity of the ellipse is close to $\sqrt{3}$ remains obscure.

Let us suppose that the respective difficulties of either of the loop models were resolved by a new loop model having correct profile and particle dynamics within the loop and another $p = 0$ surface to model the rear of the wave. (For this surface to be a true free surface we also require $\mathrm{D}p/\mathrm{D}t = 0$ on $p = 0$, which is very difficult to satisfy in general.) For this surface to connect with the loop free surface the pressure gradient, and hence the particle acceleration, would have to vanish at the point of connection (acceleration $= g$ in the fixed frame). This does not appear to have been observed in the numerical studies of breaking waves (except when the jet is very well developed). Hence such loop models are at best only partially relevant to breaking waves, a fact also pointed out by Longuet-Higgins (1982). The implication of this, that models of the loop must also take account of the jet region if they are to incorporate the rear of the wave properly, is not accommodated in the existing loop models but will be exploited in the present paper. Consequently we need to consider the region of sharp curvature around the jet described in the next section.

4. SemiLagrangian representation of the rotating hyperbolic flow

In the Eulerian representation Longuet-Higgins (1980) gives the form of a rotating hyperbolic flow, representing the jet of a plunging breaker, as

$$\chi = \tfrac{1}{2}Az^2, \tag{4.1}$$

where $A = \alpha(t)\,\mathrm{e}^{\mathrm{i}\sigma(t)}$ is a complex function of time.

Longuet-Higgins (1982) shows that in the semiLagrangian description the same flow may be represented by

$$z = F(t)\cosh\omega + G(t)\sinh\omega, \tag{4.2}$$

where $F(t)$ and $G(t)$ are chosen so as to annul the singularity arising at the focus of the hyperbola, thereby allowing the fluid to exist inside the jet.

For points on the surface of the hyperbola we have the result:

$$z = \left(\frac{2S}{\varpi}\right)^{\frac{1}{2}}[z^{(1)}\cosh\omega + \varpi^{\frac{1}{2}}z^{(2)}\sinh\omega], \tag{4.3}$$

where $z^{(1)}$ and $z^{(2)}$ are functions of time corresponding to $F(t)$ and $G(t)$ in (4.2), S is an arbitrary constant and $\varpi = P/\lambda^4$ is the quotient of two arbitrary constants of integration arising in Longuet-Higgins (1980). Now

$$z^{(1)} = \mathrm{i}t - 1 - \frac{\mathrm{i}\varpi}{24t^3} + \frac{\varpi}{120t^4} + \dots, \tag{4.4}$$

$$z^{(2)} = \frac{1}{2t} + \frac{\mathrm{i}}{6t^2} - \frac{1}{6t^3} - \frac{\mathrm{i}}{10t^4} + \dots. \tag{4.5}$$

Further Longuet-Higgins (1983) gives the r-function of (1.1) as

$$\begin{aligned} r &= -\varpi^{\frac{1}{2}}[\alpha(t)]^4 \\ &= -\varpi^{\frac{1}{2}}\left[\frac{1}{t^4}-\frac{2}{t^6}+\left(\frac{2\varpi}{3}+3\right)\frac{1}{t^8}-\left(\frac{16\varpi}{15}+4\right)\frac{1}{t^{10}}+\dots\right]. \end{aligned} \tag{4.6}$$

It is interesting to compare (4.6) with the r-function of New's ellipse solution:

$$r \sim \frac{1}{(t^2+1)^2}g_\omega(\omega), \tag{4.7}$$

where $g_\omega(\omega)$ is an arbitrary function of ω alone, and is shown to be irrelevant to the solutions of (1.1) by Longuet-Higgins (1976). Hence in the large-time limit

$$r \sim \frac{1}{t^4}-\frac{2}{t^6}+\frac{3}{t^8}-\frac{4}{t^{10}}+\dots. \tag{4.8}$$

For general ϖ the two series (4.6) and (4.8) coincide for the first two terms only, whereas for $\varpi \to 0$ and two r-functions become identical, as can also be seen directly from Longuet-Higgins (1980, equation (6.2)). Consequently in the large-time limit, or as $\varpi \to 0$, the ellipse solution for the loop region, and the Dirichlet hyperbola solution for the jet region, are complementary flows and, by the linearity of (1.1), may be added together to form a much more complete model of the entire overturning region. This observation is the principle result of this paper. The difficulty arises from the nonlinear condition that the singularity within the jet must still be annulled in the combined flow. After discussing the jet solution in terms of the polynomial solutions of (1.1), we show how it is possible to combine flows in the large-time limit.

5. Complementary flows to the rotating hyperbolic flow

We now consider some polynomial solutions of (1.1) with r-functions given by (4.6). Since (1.1) is linear, such flows will be complementary to the Dirichlet hyperbola solution (4.3) and indeed may be added together to form the Dirichlet hyperbola at least in the limit of large time and small ω (around the tip of the jet). Because the solutions for $z^{(1)}$ and $z^{(2)}$ given by (4.4) and (4.5) are expressed as large-time expansions, we consider the large-time approximation to the r-function of (4.6) given by the first two terms only. Thus

$$r = -\varpi^{\frac{1}{2}}\left(\frac{1}{t^4}-\frac{2}{t^6}\right), \tag{5.1}$$

which is identical with the first two terms of the ellipse solution r-function and so can be expected to be valid in the loop region also. This generates two classes of polynomial solutions given explicitly by

$$\begin{aligned} P_0 &= t, \\ P_1 &= t\omega - \mathrm{i}\varpi^{\frac{1}{2}}\left[\frac{1}{2t}-\frac{1}{6t^3}\right], \\ P_2 &= t\omega^2 - \mathrm{i}\varpi^{\frac{1}{2}}\left[\frac{1}{t}-\frac{1}{3t^3}\right]\omega - \varpi\left[\frac{1}{12t^3}-\frac{7}{90t^5}+\frac{1}{84t^7}\right], \end{aligned}$$

$$P_3 = t\omega^3 - \tfrac{3}{2}\mathrm{i}\varpi^{\frac{1}{2}}\left[\frac{1}{t} - \frac{1}{3t^3}\right]\omega^2 - \varpi\left[\frac{1}{4t^3} - \frac{7}{30t^5} + \frac{1}{28t^7}\right]\omega$$

$$+\mathrm{i}\varpi^{\frac{3}{2}}\left[\frac{1}{120t^5} - \frac{11}{840t^7} + \dots\right],$$

$$\vdots$$

$$Q_0 = 1,$$

$$Q_1 = \omega - \frac{\mathrm{i}\varpi^{\frac{1}{2}}}{2}\left[\frac{1}{3t^2} - \frac{1}{5t^4}\right],$$

$$Q_2 = \omega^2 - \mathrm{i}\varpi^{\frac{1}{2}}\left[\frac{1}{3t^2} - \frac{1}{5t^4}\right]\omega - \varpi\left[\frac{1}{60t^4} - \frac{13}{630t^6} + \frac{1}{180t^8}\right],$$

$$Q_3 = \omega^3 - \tfrac{3}{2}\mathrm{i}\varpi^{\frac{1}{2}}\left[\frac{1}{3t^2} - \frac{1}{5t^4}\right]\omega^2 - \varpi\left[\frac{1}{20t^4} - \frac{13}{210t^6} + \frac{1}{60t^8}\right]\omega$$

$$+\mathrm{i}\varpi^{\frac{3}{2}}\left[\frac{1}{840t^6} - \frac{17}{7560t^8} + \dots\right],$$

$$Q_4 = \omega^4 - 2\mathrm{i}\varpi^{\frac{1}{2}}\left[\frac{1}{3t^2} - \frac{1}{5t^4}\right]\omega^3 - \varpi\left[\frac{1}{10t^4} - \frac{13}{105t^6} + \frac{1}{30t^8}\right]\omega^2$$

$$+2\mathrm{i}\omega^{\frac{3}{2}}\left[\frac{1}{420t^6} - \frac{34}{7560t^8} + \dots\right]\omega + 2\varpi^2\left[\frac{1}{30240t^8} + \dots\right]$$

$$Q_5 = \omega^5 - \frac{5\mathrm{i}\varpi^{\frac{1}{2}}}{2}\left[\frac{1}{3t^2} - \frac{1}{5t^4}\right]\omega^4 - \tfrac{5}{3}\varpi\left[\frac{1}{10t^4} - \frac{13}{105t^6} + \frac{1}{30t^8}\right]\omega^3$$

$$+5\mathrm{i}\varpi^{\frac{3}{2}}\left[\frac{1}{420t^6} - \frac{34}{7560t^8} + \dots\right]\omega^2 + 10\varpi^2\left[\frac{1}{30240t^3} + \dots\right]\omega$$

$$\vdots \tag{5.2}$$

all expressions being correct to $O(t^{-8})$. For small ω the Dirichlet hyperbola solution of (4.3) is simply

$$z = \mathrm{i}(P_0 + \tfrac{1}{2}P_2) - (Q_0 + \tfrac{1}{2}Q_2), \tag{5.3}$$

with the singularity within the jet annulled to $O(t^{-5})$. Using only the first term of (4.6) to generate polynomial solutions gives the same result as (5.3) for the jet, except that the singularity is annulled only to $O(t^{-3})$. By taking more terms in (4.6) to generate the polynomial solutions we can approximate the Dirichlet hyperbola solution, which has its singularity annulled to arbitrarily high inverse powers of time, by adding higher order polynomial solutions to (5.3). For example, with the first three terms of (4.6) used to generate new polynomial solutions, we see that (5.3) still has its singularity annulled only to $O(t^{-5})$. We can, however, annul this singularity to $O(t^{-6})$ by addition of a term in P_4:

$$z = \mathrm{i}(P_0 + \tfrac{1}{2}P_2) - (Q_0 + \tfrac{1}{2}Q_2) + B_4P_4, \tag{5.4}$$

where $B = \frac{1}{24}\mathrm{i}$. This corresponds to taking the next term in the expansion of $\cosh\omega$ in (4.3), and so, by addition of higher-order polynomial solutions, to annul the singularity to higher inverse orders of time, we recover the hyperbolic solution (4.3) again. In this paper, however, we confine ourselves to the simpler flows generated

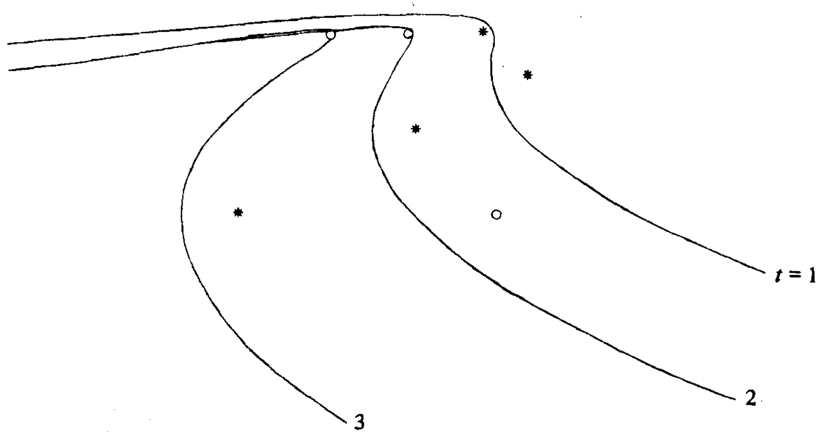

FIGURE 2. Surface profile of the breaking wave generated by (6.1). The flow has two singularities, marked * where $z_\omega = 0$, whilst $z^*_{\omega t} = 0$ is marked by $\odot$. For large time the singularity within the jet is annulled whilst the other non-annulled singularity lies outside the fluid within the loop of the wave.

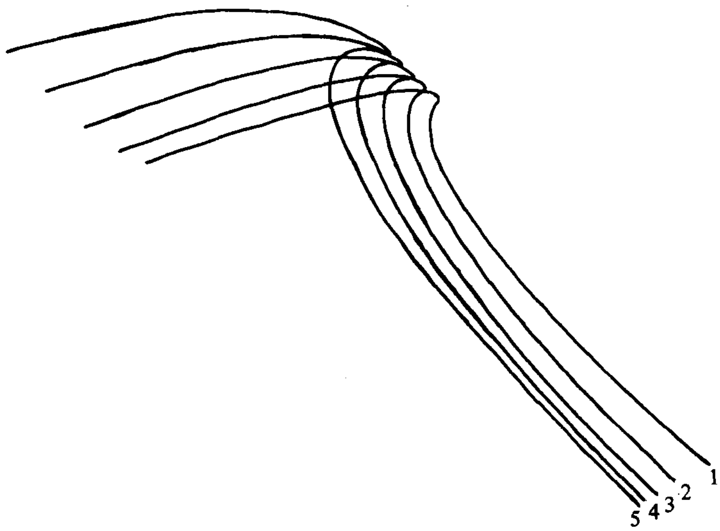

FIGURE 3. Spilling-breaker profiles for $t = 1, \ldots, 5$.

by the r-function of (5.1) with (5.3) as our model for the jet. The higher-order polynomial solutions of (5.2) will be added to this jet flow in §6 in order to model the loop and rear of the wave.

6. Addition of other polynomial solutions to the jet

We now consider other polynomial solutions with $r = -\varpi^{\frac{1}{2}}(t^{-4}-2t^{-6})$ given by (5.2), and try to model the rest of the wave by adding them to the jet of (5.3). Suppose

$$z = \mathrm{i}(P_0+\tfrac{1}{2}P_2) - (Q_0+\tfrac{1}{2}Q_2)+A_3 Q_3, \tag{6.1}$$

where A_3 is a constant.

This flow has two singularities now, one of which is not annulled but lies in the

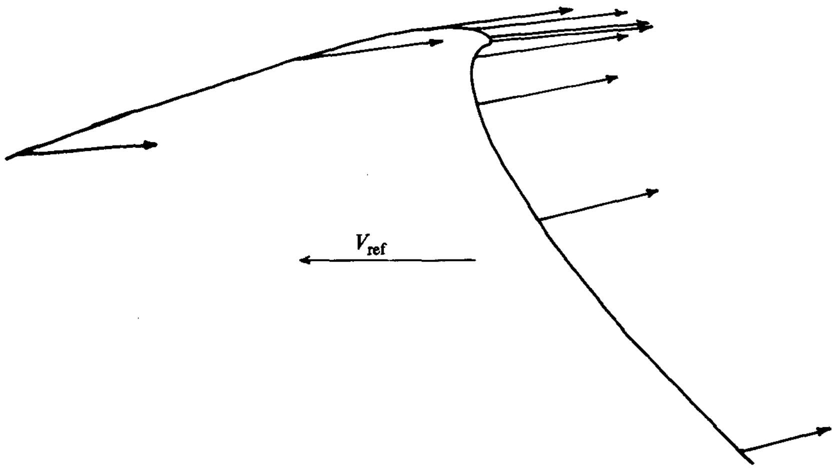

FIGURE 4. Spilling breaker velocities for $t = 2.0$ when seen in a frame of reference with instantaneous velocity V_{ref}.

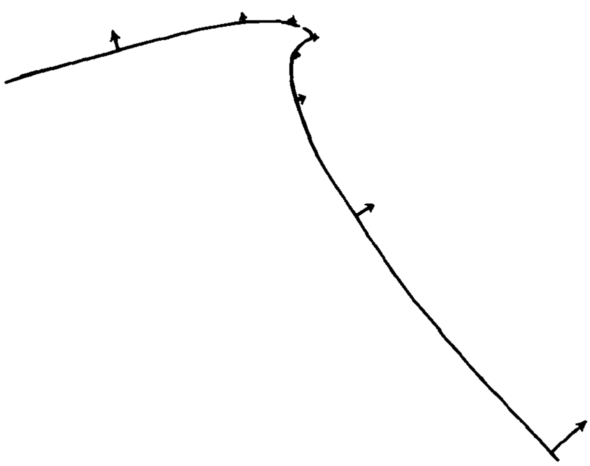

FIGURE 5. Spilling-breaker accelerations seen in the gravity-free frame for $t = 2.0$.

loop of the wave outside the fluid, and another in the jet which is annulled since $z^*_{\omega t} = 0$ when

$$\omega = \frac{\varpi^{\frac{1}{2}}}{2}\left[\frac{\mathrm{i}}{t^2} + \frac{2}{3t^3} - \frac{\mathrm{i}}{t^4} - \frac{4}{5t^5}\right] - \frac{6\mathrm{i}A_3^*\,\varpi}{5t^5}. \tag{6.2}$$

Substituting (6.2) into the expression for z_ω gives

$$z_\omega = \frac{\varpi}{t^4}\left[-\tfrac{3}{10}A_3 + \frac{6A_3^*}{5}\right]. \tag{6.3}$$

Evidently this cannot vanish for any non-vanishing A_3, and so the singularity is not annulled to $O(t^{-5})$ as with (5.3). Consistent to $O(t^{-4})$ we may write (6.2) as

$$\omega = \frac{\varpi^{\frac{1}{2}}}{2}\left[\frac{\mathrm{i}}{t^2} + \frac{2}{3t^3} - \frac{\mathrm{i}}{t^4} - \frac{4}{5t^5}\right], \tag{6.4}$$

showing that the singularity is, in fact, annulled to $O(t^{-4})$. The free-surface profiles, shown in figure 2, look very suggestive when $A_3 = \frac{1}{2}\mathrm{i}$ and the free surface asymptotes

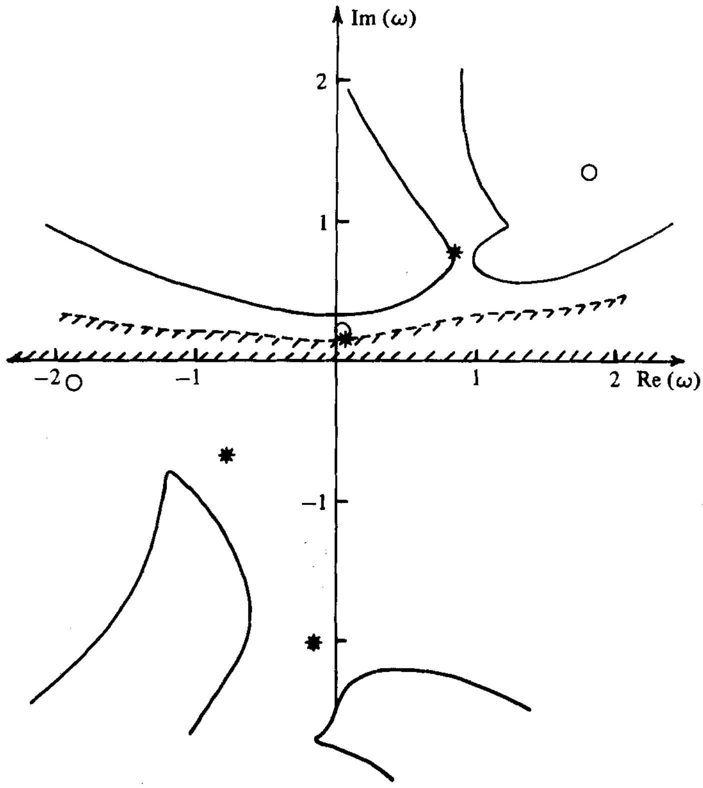

FIGURE 6. ω-plane of the fifth-order polynomial (6.7). The singularities ($z_\omega = 0$) are marked *, whilst places with $z^*_{\omega t} = 0$ are marked ⊙. The branch cut is shown dotted and the fluid lies within the shaded area. Contours other than the real ω-axis which also map to the free surface profile are shown also. $t = 2.0$.

to two 'horizontal' lines, the rear face of the wave being higher than the front face. We note, however, that the flow is essentially gravity-free, and consequently for large times the jet does not intersect the free surface on the front face of the wave, but becomes thin and horizontal. Further, for early times $t < \sqrt{2}$, the r-functions and hence the accelerations change sign and the acceleration vectors point inwards to the fluid instead of outwards as for large times. Evidently, then any combination of the polynomial solutions of (5.1) can only model the wave properly for large time, earlier times requiring more terms in the expansion of the r-function (4.6).

What will be the effect of adding additional polynomial solutions to the expression (6.1)? Q_0 and P_0 merely shift the origin and were included only to bring out the similarity with the hyperbola solution of (4.3), whilst Q_1 and P_1 when chosen so that the singularity is still annulled merely shift the surface particles along the free surface under the translation $\omega \to \omega +$ constant. For

$$z = \mathrm{i}(P_0 + \tfrac{1}{2}P_2) - (Q_0 + \tfrac{1}{2}Q_2) + A_1 Q_1 + B_1 P_1 + A_3 Q_3, \tag{6.5}$$

and non-vanishing B_1, the annulled singularity requirement implies that B_1 is pure imaginary and $A_3 B_1 = -\tfrac{1}{3}\mathrm{i}$, thereby annulling the singularity to $O(t^{-3})$. A_1 is left undetermined. This flow, however, has the jet projected perpendicularly at large times from the free-surface asymptotes, and thus does not model a plunging breaker.

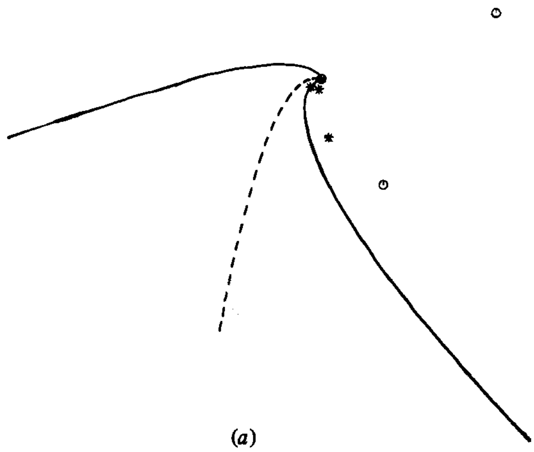

(*a*)

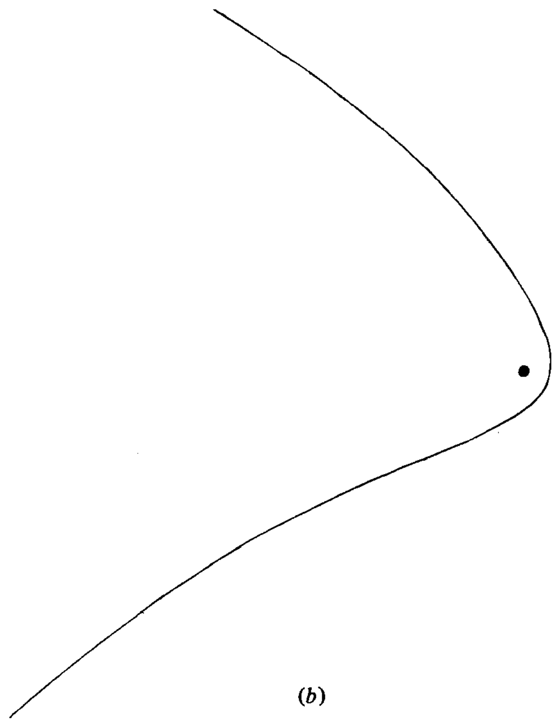

(*b*)

FIGURE 7. (*a*) z-plane of the fifth-order polynomial (6.7) showing the free-surface branch cut (dotted) and vanishing of z_ω and $z^*_{\omega t}$ as in figure 6. (*b*) Close up of the jet region of (*a*) showing the annulled singularity. Although the points where $z_\omega = 0$ and $z^*_{\omega t} = 0$ are distinct in the ω-plane (see figure 6) these points are indistinguishable at this scale when mapped to the z-plane under (6.7).

Now consider

$$z = \mathrm{i}(P_0+\tfrac{1}{2}P_2)-(Q_0+\tfrac{1}{2}Q_2)+B_3 P_3. \tag{6.6}$$

This flow has the jet singularity annulled to $O(t^{-3})$ only and hence is not as exact as (6.1). Furthermore, since we require the particle velocities to be highest in the jet region, it seems necessary to exclude all the P-type polynomial solutions when modelling the rest of the wave.

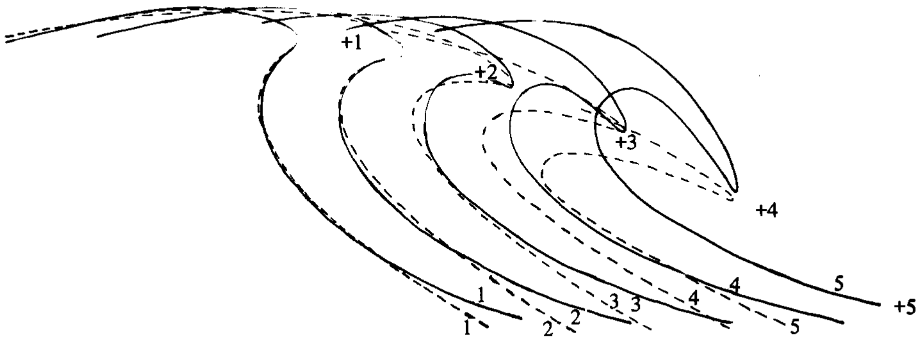

FIGURE 8. Comparison of numerical results of Vinje & Brevig (1982, private communication) (solid line) with (6.7) (dashed line). The origin (+) moves in a parabola under gravity, and the numbers indicate time.

By considering the asymptotic behaviour of the free surface for large ω we see that the next possible refinement to modelling the rest of the wave is

$$z = A[\mathrm{i}(P_0+\tfrac{1}{2}P_2)-(Q_0+\tfrac{1}{2}Q_2)]+A_3Q_3+A_4Q_4+A_5Q_5, \qquad (6.7)$$

the singularity within the jet still being annulled to $O(t^{-4})$, and the coefficient $A = a\mathrm{e}^{\mathrm{i}\theta}$ being included for convenience so that the relative size and orientation of the jet may be altered easily. With $A = \mathrm{e}^{\frac{1}{4}\mathrm{i}\pi}$, $A_3 = \frac{1}{2}\mathrm{i}$, $A_4 = -\frac{1}{2}\mathrm{i}$ and $A_5 = -0.2$ we obtain a fairly realistic representation of a 'spilling' breaker with a small overturning region, from when the wave has just overturned until when the jet is well developed (see figure 3). Again the jet does not intersect the free surface, since we have neglected gravity, but rather tends to 45°. Nevertheless, over a limited duration of time we may be entitled to ignore gravity for the reasons given in §2. The velocities of the free-surface particles, seen in an appropriate frame of reference, and shown in figure 4 for a particular time, look realistic since the jet velocities are higher than the front of the wave. On the other hand, the accelerations seen in the gravity-free frame (figure 5) are not entirely correct, since although they are in the correct direction we do not have maximum acceleration in the loop of the wave.

Since z is now given by a fifth order polynomial in ω we will have four branch points ($z_\omega = 0$) in the flow. These are shown for a particular time in figures 6 and 7 in the ω-plane and z-plane respectively. In the jet we have an annulled singularity as expected, but also in the fluid we have another apparent singularity which is not annulled. This singularity, however, is not in the fluid domain as can be seen from figures 6 and 7. In figure 7 we have drawn a branch cut from the jet singularity, the fluid lying on either side of this cut. The line of the branch cut is irrelevant so long as it is non-intersecting and completely within the fluid. In the ω-plane (see figure 6) we have plotted points which map to this branch cut under the mapping of (6.7). The fluid region, shown shaded, lies under this surface and above the real ω-axis; clearly the other singularity must lie on another Riemann surface and not in the fluid, and therefore has no significance for the flow. Also shown in figure 6 are the surfaces in the ω plane other than $\mathrm{Re}\,(\omega) = 0$ which map to the same free surface under (6.7). The singularity in question lies close to one of these surfaces. Finally, we note that within the fluid the velocity gradient $W_z = Z^*_{\omega t}/Z_\omega$ is everywhere finite, even at the annulled branch point, and so the fluid motion is everywhere continuous.

We are now in a position to attempt a fit to Vinje & Brevig's (1982, private communication) 'plunging' breaker numerical results by choosing the coefficients as follows:

$$A = 2.5\,\mathrm{e}^{\frac{1}{4}\mathrm{i}\pi}, \quad A_3 = 0.6\mathrm{i}, \quad A_4 = -0.5\mathrm{i}, \quad A_5 = -0.3-0.03\mathrm{i}.$$

A comparison of the numerical and analytic profiles is given in figure 8 showing qualitative agreement over a limited time. For the analytic results we have plotted $t = 1, \ldots, 5$, with origins moving in a parabola under the influence of gravity. Hence the flow contains gravity in a non-essential way, as explained in §2. Thus, whilst the tip falls under gravity, it does not arch over in the correct fashion and intersect the front of the wave, because in this model the front of the wave also falls under gravity. As explained in §2, including gravity in such a non-essential way can only be justified for a region close to the overturning crest. Furthermore, away from the crest region, the wave is essentially progressive. For steady progressive waves Longuet-Higgins (1982) points out that the r-function will be a function of $\omega - t$, which therefore cannot be factorized as $r(\omega, t) = T(t)\, W(\omega)$ as in the present paper. This is further discussed in §7, where the progressive nature of the numerical r-function is clearly exhibited. Evidently then, the above model is strictly limited to the local region of the loop and jet of the wave, but does provide a qualitative model of the overturning process.

The velocity profiles of the surface particles of this plunging breaker, when seen in the accelerated reference frame used above also look realistic (see figure 9) except for $t = 1$, where the velocities on the forward face of the wave are greater than in the jet, and on the rear face where the velocities have substantially incorrect directions (upwards instead of towards the jet.) We can hardly expect the velocities and accelerations to be correct for $t = 1$ since the theory is only valid for large times ($t \geqslant 2$), when the singularity within the fluid is annulled accurately. In fact, for $t = 2$ the spilling breaker ($A = \mathrm{e}^{\frac{1}{4}\mathrm{i}\pi}$, $A_3 = \frac{1}{2}\mathrm{i}$, $A_4 = -\frac{1}{2}\mathrm{i}$, $A_5 = -0.2$) has $z_\omega = 0$ when $z = -2.1334+\mathrm{i}0.72885$, whilst $z^*_{\omega t} = 0$ when $z = -2.1319+\mathrm{i}0.72795$, and for the plunging breaker ($A = 2.5\,\mathrm{e}^{\frac{1}{4}\mathrm{i}\pi}$, $A_3 = 0.6\mathrm{i}$, $A_4 = -0.5\mathrm{i}$, $A_5 = -0.3-0.03\mathrm{i}$) $z_\omega = 0$ when $z = -5.3342+\mathrm{i}1.8225$, whilst $z^*_\omega t = 0$ when $z = -5.3327+\mathrm{i}1.8207$, showing that the singularity is annulled very accurately even for moderate times.

The particles move up the front face of the wave as required. The accelerations, however, do not reach a maximum in the node of the wave, but increase monotonically with distance away from the jet as expected from the clustering of the particles there (z_ω is small) and (1.1).

In New (1983) some very accurate calculations of the free surface with 180 points per wavelength reveal a jet which does not curl down as much as the jet in the calculations of Vinge & Brevig (1980) but is qualitatively similar to the proposed analytic solution with $A = 3.5\,\mathrm{e}^{\frac{1}{4}\mathrm{i}\pi}$, $A_3 = 0.7\mathrm{i}$, $A_4 = -0.5\mathrm{i}$ and $A_5 = -0.35$. Figure 10 shows a comparison of the two results with the axis moving in a suitable free-fall trajectory. Although the agreement is better than figure 8, we see clearly that any improvement in the theory must take account of gravity in a non-trivial fashion, as well as the progressive nature of the rest of the wave.

7. Consideration of the numerical solution of Vinje & Brevig

From the numerical calculations of Vinje & Brevig (1982, private communication) we know the accelerations of the surface particles and their positions as the wave breaking progresses. As explained in Longuet-Higgins (1976) we can label the free-surface particles arbitrarily; thus imagining the particles to be labelled by integer

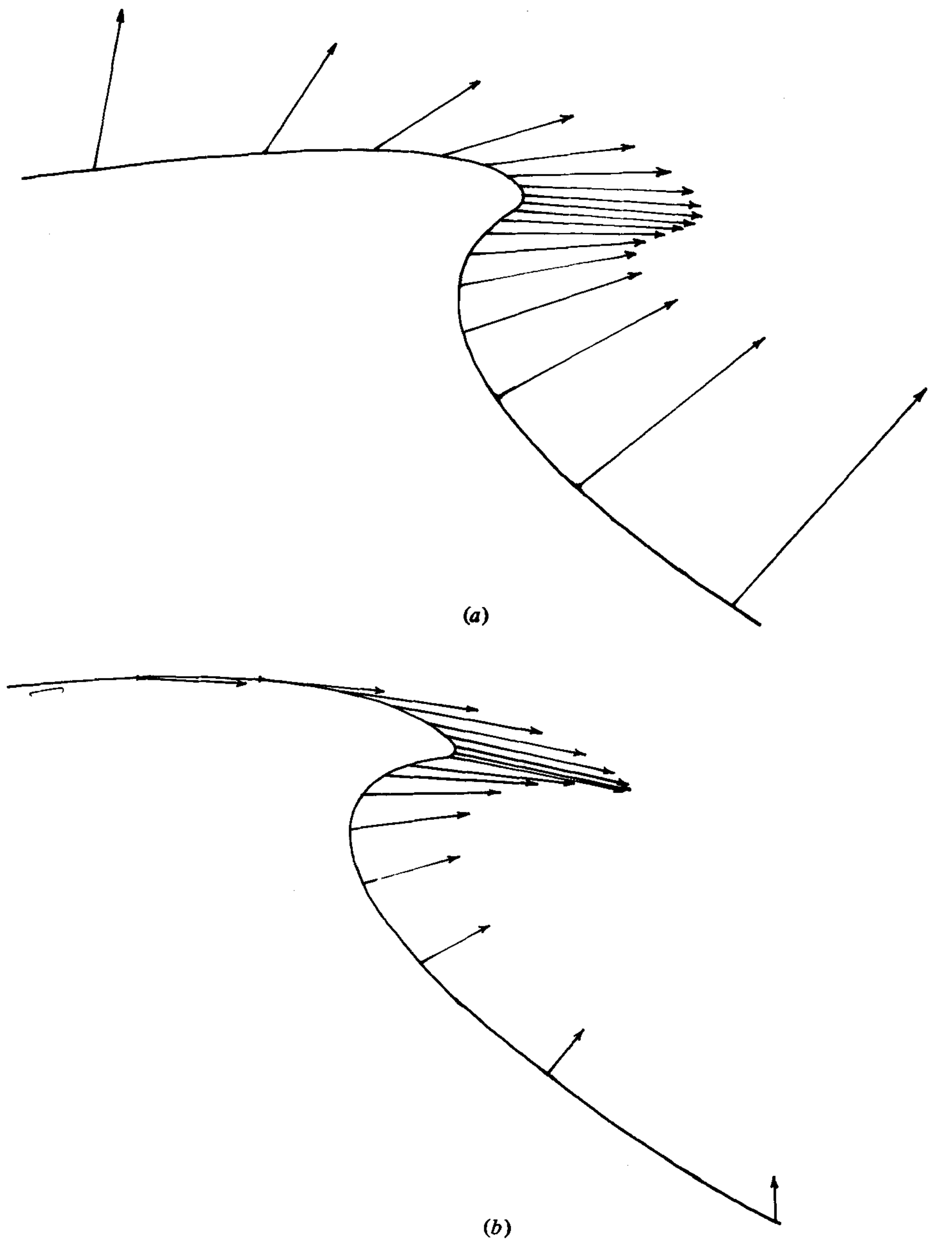

FIGURE 9 (a, b). For caption see facing page.

values of ω say, we can calculate z_ω and consequently the r-function from (2.1). Figure 11 shows the r-function as a function of time for various labelled particles as they move up through the node of the wave, where the r-function is close to its maxima, and into the jet where the r-function falls rapidly. Because of the progressive nature of the rest of the wave, which must have $r(\omega - t)$, the labelled particles do not enter the breaking region simultaneously, and consequently the fitted curves of

$$r \propto \frac{-1}{[1+[t-t_0(\omega)]^2]^2}, \tag{7.1}$$

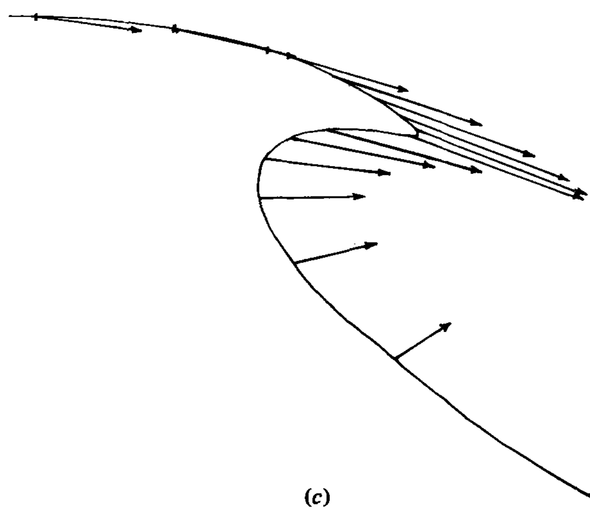

(*c*)

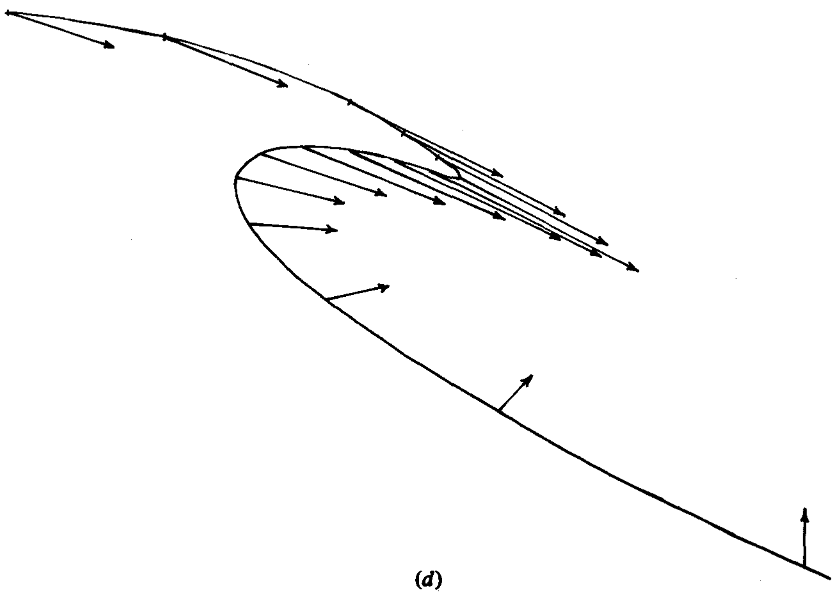

(*d*)

FIGURE 9. Velocities of the surface particles when seen in the appropriate accelerating reference frame: (*a*) $t = 1.0$; (*b*) 2.0; (*c*) 3.0; (*d*) 4.0.

(shown dotted in figure 11) must each have a different time origin $t_0(\omega)$. It also appears necessary to have the time-scale dependent upon ω. However, for any particular particle, the time dependence of the r-function would appear to be modelled quite well by (7.1) as the particle passes through the loop and into the jet of the wave. The same comment applies to particle 22 (see figure 11), which passes up the near vertical face and onto the top of the wave before the jet is ejected, although the agreement does not appear to be so good.

From the numerical solution we may therefore conclude that a local model of the crest of a breaking wave generated by the r-function of (7.1) may indeed have a time development that is approximately correct.

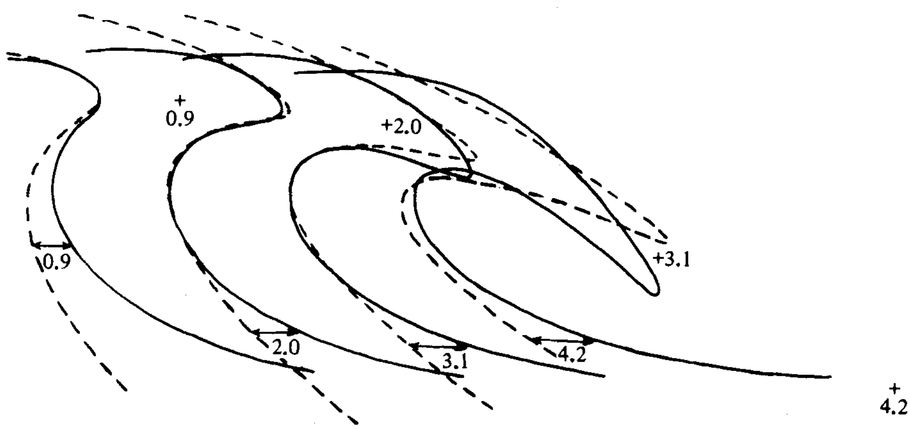

FIGURE 10. Comparison of numerical results of New (1983) (solid line) with (6.7) (dashed line). The origin (+) moves in a parabola under gravity, and numbers indicate time.

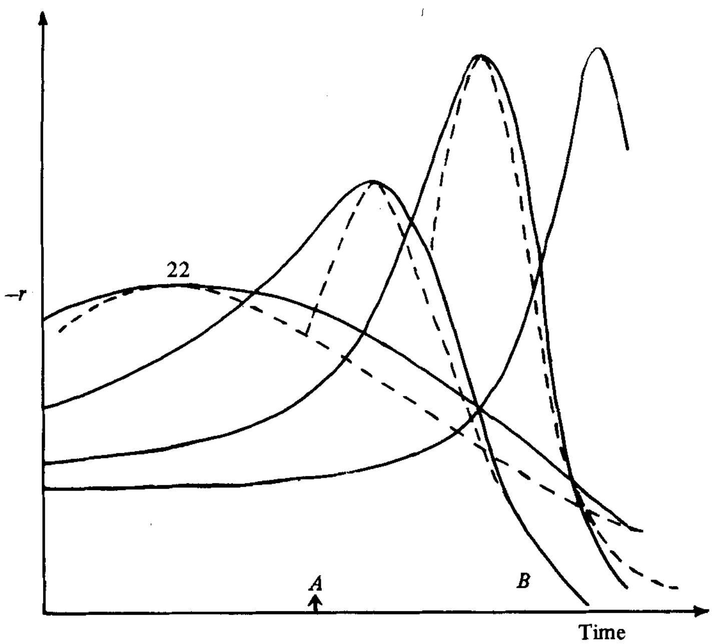

FIGURE 11. Numerically generated r-function compared with that of (7.1). Solid lines are from the numerical results of Vinje & Brevig (1982, private communication); dashed lines indicated the analytic r-function of (7.1). A indicates when the front face of the wave becomes vertical, whilst B denotes times when the jet is well formed.

8. Conclusion

A weakness of both the cubic-polynomial model of Longuet-Higgins (1982) or the $\sqrt{3}$-ellipse of New (1982) is that it does not appear possible to account for the jet or the rear of the wave in a proper fashion. Both models include at least one singularity within the loop, but it appears necessary to include a singularity within the fluid (in the jet) in order to make the free surface curl back to form the rear of the wave. A model having this feature is the semiLagrangian description of the Dirichlet hyperbola (Longuet-Higgins 1983) which has, for large time, the same r-function as the $\sqrt{3}$-ellipse solution of New (1982). This implies that solutions generated with this r-function could be relevant, not only at the jet, but also around the loop of the wave. Such a model has been described which gives the forward face, loop, jet and rear of the wave in a fairly realistic way, and comparisons with the numerical breaking-wave profiles of Vinge & Brevig (1982, private communication) and New (1983) look encouraging.

I wish to thank Professor M. S. Longuet-Higgins for his discussion and helpful comments, Professor Tor Vinje and Per Brevig for the results of their numerical computations and Adrian New for discussion about ellipses and numerical results. I would also like to thank the Royal Society for funding me under Professor Longuet-Higgins' research grant, and the referees of this paper for their helpful criticisms.

REFERENCES

JOHN, F. 1953 Two-dimensional potential flows with a free boundary. *Communs Pure Appl. Maths* **6**, 497–503.

LONGUET-HIGGINS, M. S. 1976 Self-similar flows with a free surface. *J. Fluid Mech.* **73**, 603–620.

LONGUET-HIGGINS, M. S. 1980 On the forming of sharp corners at a free surface. *Proc. R. Soc. Lond.* A **371**, 1980 453–478.

LONGUET-HIGGINS, M. S. 1981 Advances in breaking-wave dynamics. In *Proc. IUCRM Symp. on Wave Dynamics, Miami Beach, Florida, May 1981.*

LONGUET-HIGGINS, M. S. 1982 Parametric solutions for breaking waves. *J. Fluid Mech.* **121**, 403–424.

LONGUET-HIGGINS, M. S. 1983 Rotating hyperbolic flow: particle trajectories and parametric representation. *Q. J. Mech. Appl. Maths* **36**, 247–270.

NEW, A. 1982 *Contribution to IAHR Symp. on Non-linear Waves, Delft, 22–23 April, 1982.*

NEW, A. 1983 A class of elliptical free-surface flows. *J. Fluid Mech.* **130**, 219–239.

VINJE, T. & BREVIG, P. 1980 Breaking waves on finite water depths: a numerical study. *Ship Res. Inst. of Norway* R-118.81.